Demulsification of MIRI Crude Emulsion using Aeration

by

Amirul Ariffin Bin Ahmad Zahidin

14798

Dissertation submitted in partial fulfillment of the requirements for the

Bachelor of Engineering (Hons)

(Mechanical)

JANUARY 2015

Universiti Teknologi PETRONAS

32610 Bandar Seri Iskandar

Perak Darul Ridzuan

CERTIFICATION OF APPROVAL

Demulsification of MIRI Crude Emulsion using Aeration

by

Amirul Ariffin Bin Ahmad Zahidin

14798

Dissertation submitted in partial fulfillment of the requirements for the

Bachelor of Engineering (Hons)

(Mechanical)

JANUARY 2015

Approved by:

_____

Dr. Azuraien Bt. Japper @ Jaafar

Universiti Teknologi PETRONAS

32610 Bandar Seri Iskandar

Perak Darul Ridzuan

CERTIFICATION OF ORIGINALITY

This is to certify that I am responsible for the work submitted in this project, that the original work is my own except as specified in the references and acknowledgement, and the original work contained herein have not been undertaken or done by unspecified sources or persons.

_____

AMIRUL ARIFFIN BIN AHMAD ZAHIDIN

ABSTRACT

Throughout the oil production, crude oil emulsification is inevitable and become major challenges. The emulsification effect in operational problem especially pressure drop, low flow rate, increase in demulsifier dosage and low production. One of the potential technique in demulsifying the emulsion is by aeration. This report present the findings of a series of experiments performed to analyze the separation of emulsion, water and oil after aeration treatment at different volumetric flow rate of 50cc/min, 100cc/min, 150cc/min and 200cc/min. The different sizes of bubbles resulted from three orifice diameter used; 1mm, 3mm and 6mm. The different sizes of bubbles affect the demulsification rate affected by the hydrodynamic force as the bubble rises. From the findings, the best aeration rate is 100cc/min using 1mm diameter observed at the critical 30th minutes. The optimum solution resulting in separation of approximately 47% oil fraction 30% water fraction and only 25% emulsion layer.

ACKNOWLEDGEMENT

TABLE OF CONTENTS

LIST OF FIGURES

LIST OF TABLES

CHAPTER 1:

INTRODUCTION

1.1 Background

In today's petroleum production, many challenges must be faced such as the high pumping cost, piping corrosion and low flow rate mainly due to the formation of the water-in-oil (W/O) emulsion throughout the production. The cause of the emulsion has been identified to be due to the natural surfactant i.e. asphaltenes, waxes, resins (Schramm, 2005) and also the mixing energy of the production processes.

Studies on demulsification have been growing throughout the years. However, there is still a huge potential of research and studies to tackle the problem of demulsification of the stubborn emulsion that still troubling the industry. By understanding the formation of the emulsion, the separation process efficiency can be increased. One of the potential techniques is by aerating the emulsion to increase the density difference and subsequently encouraging separation.

Therefore, this study is aimed to address this fundamental aspect by analyzing the stability crude emulsion, carrying out demulsification study and determining the rate and mechanism of demulsification process via aeration.

1.2 Problem Statement

During production in an oil and gas field, the hydrocarbon which is composed of oil, gas and brine (produced water) will be produced together from the well. In the pipe, they commingle during flow in the pipeline before reaching the surface production facilities. Emulsion may form due to the mixing energy caused by the bend of the pipe, the choke valves and also by the pump or the compressor.

The formation of stable crude emulsion has been identified as one of the problems in the production of the crude oil. By understanding the formation of emulsion and stability of the emulsion, the strategy can be planned and devised to break the emulsion. One of the method is via aeration.

1.3 Objectives and Scope of Study

The objectives of the study are;

1. To explore and investigate the performance of aeration for demulsification process.
2. To determine optimum aeration rate for optimum emulsion separation.
3. To access the effects of aeration bubble size on the emulsion separation.

The scope of the study for the emulsion is water-in-oil (W/O) type of macro emulsion. The emulsion is commonly found in the production field. The typical droplet sizes exceed 10μm (Becher P., 2001). The study is carried out fully experimental in the lab.

CHAPTER 2:

LITERATURE REVIEW

2.1 Emulsion Classification

Emulsion have been greatly studied due to their widespread occurrence in everyday life and nature surroundings. They have been found in many areas such as food, cosmetics, pharmaceutical and agricultural industry. One that is greatly debated for decades is the petroleum emulsions. It is typically undesirable because it can give impact to the petroleum industry resulting in pipeline corrosion, low flow rate, reduced throughput and low production. Throughout the whole oil and gas processes, emulsions is present in transporting, drilling, refinery and production of the hydrocarbon.

Emulsion is a mixture of two immiscible liquids usually defined as oil and water. One of the liquid is dispersed immiscibly in another continuous liquid in an emulsion system and it is not thermodynamically stable. The crude oil emulsion is formed when oil and water come onto contact when there is sufficient mixing energy with or without the presence of the emulsifying agent.
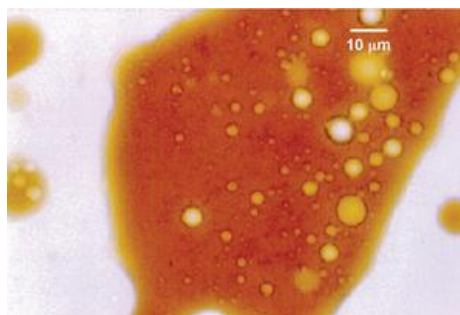
Figure 1: Water-in-Oil (W/O) Emulsion

In the petroleum industry, the two common phase of emulsion encountered are the water-in-oil (W/O) emulsion and the inverse phase namely oil-in-water (O/W) emulsion. It is also stated from Schramm (2005), the emulsification technique i.e. the applied shear force and the oil-water ratio can determined the final type of emulsion than the surfactants itself. It shows the emulsification method and oil-water ratio are critical in emulsion formation.

2.2 Emulsion Stability Mechanism

2.1.1 Sedimentation and Creaming

Sedimentation or creaming is due to the differences in densities between a continuous phase and the dispersed phase resulting in producing two separate dispersion layers as well as different phases. It may not result in emulsion breaking but it promote coalescence by increasing the droplet accumulation and result in higher probability of droplet-droplet collisions (Schramm, 2005). Creaming is the opposite of sedimentation but the principle is the same where it creates a droplet concentration gradient leading to close packing of droplets.

The driving force, Fg is the gravity phenomena for sedimentation and creaming;

$$Fg = mg - v(\rho_2 - \rho_1)g$$
$$= (4/3) \pi a^3 (\rho_2 - \rho_1)g$$

(Schramm, 2005)

Whereas,

a = droplet radius (m)

ρ_2 = droplet density (kg/m^3)

ρ_1 = the continuous phase density (kg/m^3)

g = 9.81m/s^2

m = droplet mass (kg)

v = droplet velocity (m^2/s)

However, the density difference of oil and water alone may not break the emulsion. An emulsion pad or a rag layer is an unresolved emulsion even after series of treatments. Their presence may cause several problems such as occupying more space in separation tank, increase in residual oil in treated water, increase in Basic Sediment & Water (BS&W) of the treated oil and acting as barrier for water droplets/solids to further separate.

5

2.1.2 Flocculation or aggregation

Flocculation is the process in which emulsion droplet aggregate and touching each other without the particle fusing together. Ivanov (1999) added that the flocculation process will clump the droplets together or aggregate whilst retaining the interfacial film. In aggregation or flocculation, two or more droplets only touching at certain points and clump together and in microscopic view, virtually no change in total surface area. The rate of flocculation depends on the temperature of emulsion, viscosity of the oil and also the density. The droplets retain their identity but lose their kinetic independence because the aggregation moves in a single unit. Flocculation of droplets may lead to coalescence and initiate the formation of larger droplets until the phase becomes separated.

The rate of flocculation depends on different factors. For instance, high temperature increases the thermal energy of the droplets and increases their collision which helps flocculation rate. There is also the usage of electrostatic field to increase the movement of the droplets of different charge toward the electrode which they aggregate.
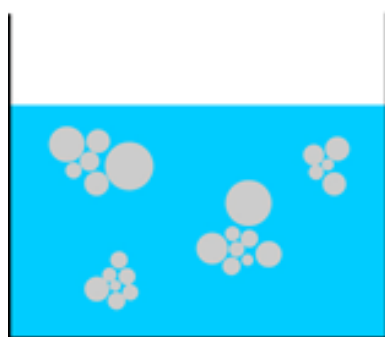
Figure 2: Flocculation of droplets

2.1.3 Coalescence

In coalescence, two or more droplets fuse together to form a single larger unit with a reduced total surface area. Schramm (2005) defined coalescence as the reducing total number of dispersed droplets and the total interfacial area between phases. The reducing total interfacial area mainly contributed by the merging of two or more dispersed droplets into a single larger unit. In emulsions and foams coalescence can lead to the separation of a macro phase, in which case the emulsion or foam is said to break. The coalescence for solid particles is called sintering.

The rate of coalescence depends on many factors such as the high rate of flocculation where it increases the collision frequency between the droplets. In addition, high interfacial tension will reduce its interfacial free energy by coalescing. High water cut also increases the collision frequency between the droplets. The addition of chemical demulsifiers and high temperature also promotes coalescence by converting solid films around droplets into a weak films and reducing the viscosities respectively.
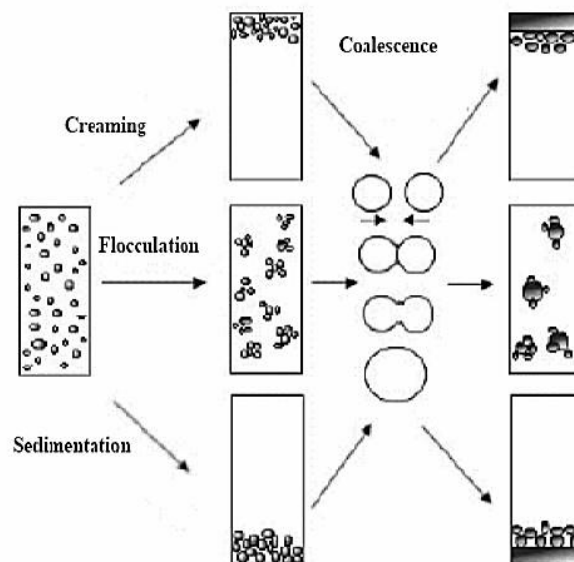
Figure 3: Processes taking place in emulsion leading to
emulsion separation and breakdown (Auflem, 2002)

2.1.4 Ostwald Ripening

The Ostwald ripening is defined as the molecular diffusion which comes from the solubility differences i.e. the oil contained within the different droplet sizes. According to Kelvin equation, the decreasing size will increase the solubility of substance in spherical particle.

$$c(r) = c(\infty)\exp\left(\frac{2yVm}{rRT}\right)$$

Whereas;

c(r) is the aqueous solubility of oil contained within a drop of radius r

$c(\infty)$ is the solubility in a system with only a planar interface

y is the interfacial tension between two phases

Vm is the molar volume of the oil

The increased in solubility result in the smaller droplets to diffuse with the aqueous phase and becoming larger droplets. As a consequence, the emulsion drops size is increased complementary to the decrease in interfacial area providing the droplets to grow. The oil droplets is pressed together by squeezing water out of the system when the osmotic pressure is applied (J. Bibette et al., 1992)

Ostwald ripening also cause the diffusion of the droplets from smaller to larger droplets. This cause by the greater solubility of the single droplets in the larger droplets. The rate of the diffusion process is related to the solubility of the droplets in the continuous phase of the emulsion which lead to the emulsion destabilization i.e. creaming.

2.3 Methods of Demulsification

Emulsion breaking also known as demulsification is carried out by using either four methods such as mechanical, thermal, chemical and electrical. The rate of separation of the demulsification depends on the knowledge of the properties and characteristics of the emulsion as well as the coalescence of the water droplets.

2.3.1 Chemical Methods

To destabilize or assist in coalescence, demulsifiers which are of chemical compound are widely used. This is the most well-known method as it is cost effective, easy to be applied and minimizes the amount of heat and settling time.

The demulsifier is injected into the emulsion system and mixes well with the emulsion to remove the protective film around the droplets. The protective films also known as the surfactants.

2.3.2 Thermal Methods

Heating lessens the oil viscosity. Increasing temperatures bring about the destabilization of the rigid films due to diminishing interfacial viscosity. Heating accelerates emulsion breaking; but, it infrequently resolves the emulsion issue alone.

Moreover, increasing the temperature has some negative impacts such as it involve costs to heat the emulsion stream. Heating could bring about the loss of crude oil light ends, decreasing its API gravity and the treated oil volume. Lastly, heating also could increase tendency of scale deposition and corrosion in treating vessels.

2.3.3 Electrical Methods

The water droplet is polarized when there is presence of electrostatic field. The positive and negative charges of the droplets are brought adjacent to each other and coalesce. The electric field causes the droplets to move about rapidly causing higher collision of the droplets. The droplet then coalesce when they collide at enough velocity which is controlled by the voltage gradient.

Research also shows that the electrostatic field, instead of providing collision, pull the droplets apart due to voltage gradient causing a tighter emulsion. To avoid this, the voltage gradient need to be adjusted by electrostatic treaters (H.B. Bradley, 1987)

2.3.4 Mechanical Methods

The usage of mechanical method can destabilize the emulsion by agitation or shear. Agitation or shear promotes the emulsion instability as higher shear causes turbulence. SPE (2014) also concludes that turbulent flow will lead to smaller droplets size which is more stable than larger droplet size, therefore, it causing a stable and tighter emulsion in the production line.

There is a wide variety of mechanical equipment available for breaking oilfield emulsions including:

- Two- and three-phase separators: The three components (oil, water and gas) have different densities, which allows them to separate by moving slowly with gas on top, water on the bottom and oil in the middle.

- Settling tanks: The density difference between the oil and water causes the water to separate from the oil by gravity.

- Free-water knockout drums: Same principle as three-phase separator. Beneficial to separate free water from emulsion before being treated as the amount of energy required to heat the water is twice of oil.

- Desalters: It is used to remove salts and particle from crude oil. The emulsion of crude oil-brine is produced by mixing with the wash water using a mix valve. Salt is extracted from the brine to the wash water droplets and coalescence with the aid from the electric field causing lower residence time and smaller size unit. The briny water is removed from the bottom of the vessel and desalted oil from the top.

Gravitational separation usually separates oil/water by exploiting the density variations. Water has a higher density than oil, and greater tendency to settle down. The settling rate of water droplets is approximates by Stokes' Law;

$$v = \frac{2gr^2(\rho_w - \rho_o)}{9\mu},$$

Whereas:

v = the settling velocity of the water droplets

g = the acceleration caused by gravity

r = the radius of the droplets

$(\rho w - \rho o)$ is the density difference between the water and oil

μ = the oil viscosity

The Stokes' law applies when Reynolds number, Re, of the particle is less than 0.1 as higher value of Re leads to turbulent flow. The settling velocity can be increased as suggested by Stokes' Law by reducing the viscosity of the liquid, increasing the droplet size and increasing the density difference between water and oil

2.4 Demulsification: Engineering Principle

American Petroleum Institute API 12J: Specification for Oil and Gas Separators and API 12L: Specification for for Vertical and Horizontal Emulsion Treaters, specify the liquid retention time as a design criteria for separators.

Table 1: API 12J Design Criteria of Three Phase Separators

Oil Gravities	Minutes (Typical)
Above 35° API	3 to 5
Below 35° API	
100+° F	5 to 10
80+° F	10 to 20
60+° F	20 to 30

Based on the standards requirements separation is to take place within 30 minutes. For the demulsification treatment time in the emulsion treater, the specification in API 12L allows the residence time in the oil settling zone typically in the range of 30 to 100 minutes. Hence, 30 minutes is taken as the reference retention time for selection of heat treatment.

The retention time factor is affected by the oil settling time to allow adequate water removal from oil or by the water settling time to allow adequate oil removal from water. The formula for Basic Sediment and Water (BS&W) is presented as:

$$BS\&W = \frac{Fraction\ of\ a\ phase\ presence\ in\ crude\ (ml)}{Total\ volume\ of\ crude\ (ml)}$$

A phase as defined in formula above can be either oil, water or emulsion. For the experiment, BS&W for emulsion is mainly used. Nevertheless, for additional data which showcase the separated oil and emulsion quality (in percentage of BS&W) are provided as well to observe the progressions during the experiments.

2.5 The Effect of Bubble Size on Hydrodynamic Force

The rate at which water will settle due to gravitational forces is dependent on the difference in density of the oil droplet and the water, the size of the droplets (Stokes' Law), and the rheology of the continuous phase. The oil droplets rising rate is also influenced by the hydrodynamic and colloidal interactions between the droplets, the physical state of the droplets, the rheology of the dispersed phase, the electrical charge on the droplets, and the nature of the interfacial membrane (Fingas, 2005).

Wu and Gharib (2002) in their paper entitled "Experimental Studies on the Shape and Path of Small Air Bubbles Rising in Clean Water" reported that the shape and bubble size affect the hydrodynamic force where there are two types of bubble shape; spherical and ellipsoidal. Their work is also supported by Woodrow L. Shew et. al. (2006). Their study demonstrates larger ellipsoidal bubbles more than 1.5mm diameter will follow spiral path trajectory. For the same diameter of spherical bubble will have the zigzag path.

The velocity generated by the bubbles will determine the bubble shape. Wu and Gharib (2002) found that the smaller diameter capillary rise will have nearly twice the velocity of the large diameter capillary. Smaller diameter capillary has bubble curvature at detachment point as shown in Figure 8. A large initial speed is produced resulting in the ellipsoidal bubble shape. However, for larger diameter capillary will develop slower velocities due to weak perturbations from the detachment and keep the bubble retain its spherical shape.

The rising of the straight bubbles relies on the buoyancy force (F_B) and drag force (F_D) which can described by equation of motion by Woodrow et. al. (2006).

$$F_B = -F_D$$

F_B and F_D is given by,

$$F_B = (\rho_l - \rho_g)Vg$$
$$F_D = 0.5C_D \pi R^2 (\rho_l - \rho_g)U^2$$

(Woodrow et. al., 2006)

where,

$\rho_l = density\ of\ liquid\ (oil)$ (kg/m3)

$\rho_g = density\ of\ bubble\ (air)$ (kg/m3)

$V_g = volume\ of\ bubble$ (m3)

$C_D = coefficient\ of\ drag$

$R = radius\ of\ bubble$ (m)

$U = velocity\ of\ bubble$ (m2/s)

It is described by Moore (1965) where the drag coefficient C_D can be predicted for millimeter bubble size. Also, the value of H(X) and G(X) can be found from the table and equation provided by the same author.

$$C_D = \frac{48}{Re}G(X) + \frac{48}{Re^{\frac{3}{2}}}G(X)H(X)$$

(Moore, 1965)

The value of G(X) can be calculated using,

$$G(X) = \frac{\frac{1}{3}X^{\frac{4}{3}}(X^2-1)^{\frac{3}{2}}\left[(X^2-1)^{\frac{1}{2}} - (2-X^2)sec^{-1}X\right]}{\left[X^2 sec^{-1}X - (X^2-1)^{\frac{1}{2}}\right]^2}$$

(Moore, 1965)

Re is the Reynold's number of the bubble and can be obtained by,

$$Re = \frac{2RU}{v}$$

(Moore, 1965)

where,

R = bubble radius (m)

v = kinematic viscosity (m²/s)

The value of X which is the aspect ratio is expressed as the length of the semi-major axis divided by the length of the semi-minor axis. It is given by,

$$X_{(R)} = 2.18R - 0.1$$

(Woodrow et. al., 2006)

Lastly, the value of the kinetic energy delivered to the fluid as the bubble rises is given by,

$$E_k = F_B \cdot U$$

(Woodrow et. al., 2006)

Wu and Gharib (2002) stated that the size of the capillary tube where the bubble is detached will determine the shape of the bubble. Smaller diameter (0.1-0.2cm) of the tubes with aspect ratio of about 1.1 to 2.2 will generate mostly ellipsoidal shape bubble. While for larger diameter of the tube with aspect ratio ranging from 1 to 1.08 will give the shape of spherical bubble. However, Woodrow et. al., (2006) results strongly suggest that the bubble shape changes does not play a critical role to the hydrodynamics.

CHAPTER 3:

METHODOLOGY

3.1 Project Activities Flow Chart
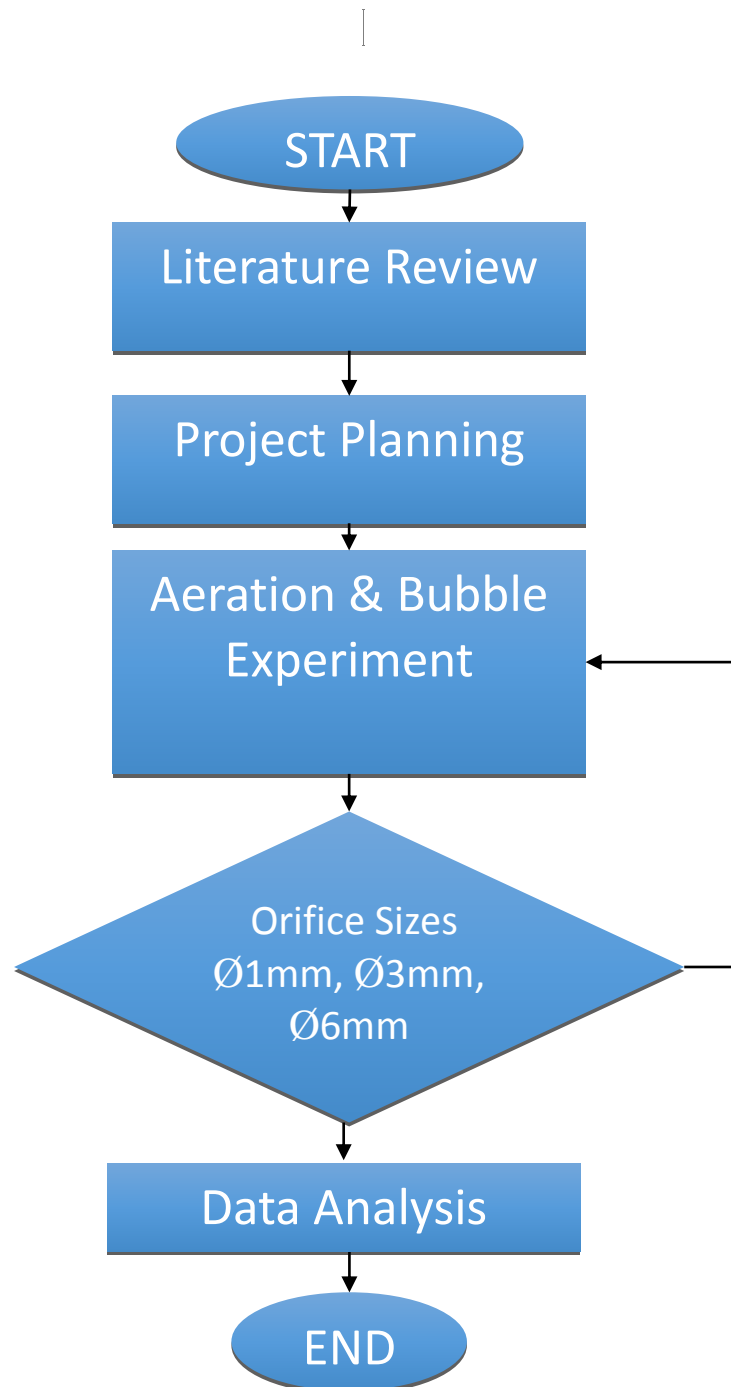
3.2 Procedures of Experiment

3.2.1 MIRI sample

The MIRI sample is obtained from the operator. Thus, the formation water is already mixed within the sample and no produced water needs to be added for this experiment.

3.2.2 Water-in-Oil Emulsion Preparation

A high speed disperser is used to create the emulsion of the sample. The high speed disperser is used instead of the overhead stirrer because it can create a tight emulsion to mimic the actual emulsion in the operation due to its high speed operation.

The mixing speed is maintained at 10000 rpm for 15 minutes during mixing. The parameter used is as per advised by the field operator and it is also mentioned that the parameter also imitated the actual operation of 743 barrel per day.

The mixture is maintained at a temperature of 60°C in a water bath mimicking actual flow line temperature.

3.2.3 The Demulsification using aeration

The demulsification process via aeration is conducted using the gas bubble emulsion unit manufactured by SOLTEQ. The unit is also known as demulsification test rig.

Before starting the demulsification treatment, the desired orifice is placed into the aeration hole. The reactor cylinder is tighten up to prevent any leakage after the emulsion is poured in. All the valves must be in close mode before starting the experiment.

After the crude emulsion is prepared, it is quickly and carefully placed inside the reactor cylinder through the top hole of the chamber unit. The crude emulsion poured put slowly to monitor any leakage in the chamber unit.

Then, the aeration source is open to allow the air inside the unit. The air is controlled using the controller and set to 50 cc/min. The emulsion is treated for 30 minutes and the behavior is carefully observed.

The treated emulsion is poured out from the chamber unit using the valve at the bottom of the reactor cylinder. The emulsion is carefully poured into a 50 mL test tube for bottle test to be carried out for the emulsion. The test tube is observed for every 5 minutes, 15 minutes, 30 minutes, 1 hour, 2 hour, 4 hour, 2nd day, 3rd day, 4th day, 5th day, 6th day, 2nd week, 3rd week and 4th week. The temperature of the treated emulsion is maintained at 60°C inside an incubator.

The maintenance of the test rig is carried out before the next experiment commences. This is to ensure the chamber unit is clean from any debris of the previous emulsion and to keep the experiment integrity. The aeration treatment steps are repeated by changing the orifice size of 3mm and 5 mm diameter respectively.

3.2.4 The Apparatus Set-up

The test is conducted by using SOLTEQ gas bubble emulsion unit model BH 29 namely as demulsification test rig. The unit must be switch on for an hour early to allow the unit to gain heat to achieve the required temperature of 60°C inside the chamber. For uniform heat distribution, it is required for the unit to be switched on at least 60 minutes prior to treatment.

The demulsification test rig can be operated with heating mode, chemical injection mode with or without aeration mode. For this study, only the aeration and heating mode are explored. Aeration is achieved by injecting air or other gases through an orifice at the bottom of the reactor cylinder. The temperature can be adjusted using the temperature controller and kept at 60°C. The temperature is measured via a temperature sensor inside the reactor cylinder.

Figure 4: SOLTEQ Gas Bubble Emulsion Unit (Demulsification test rig)
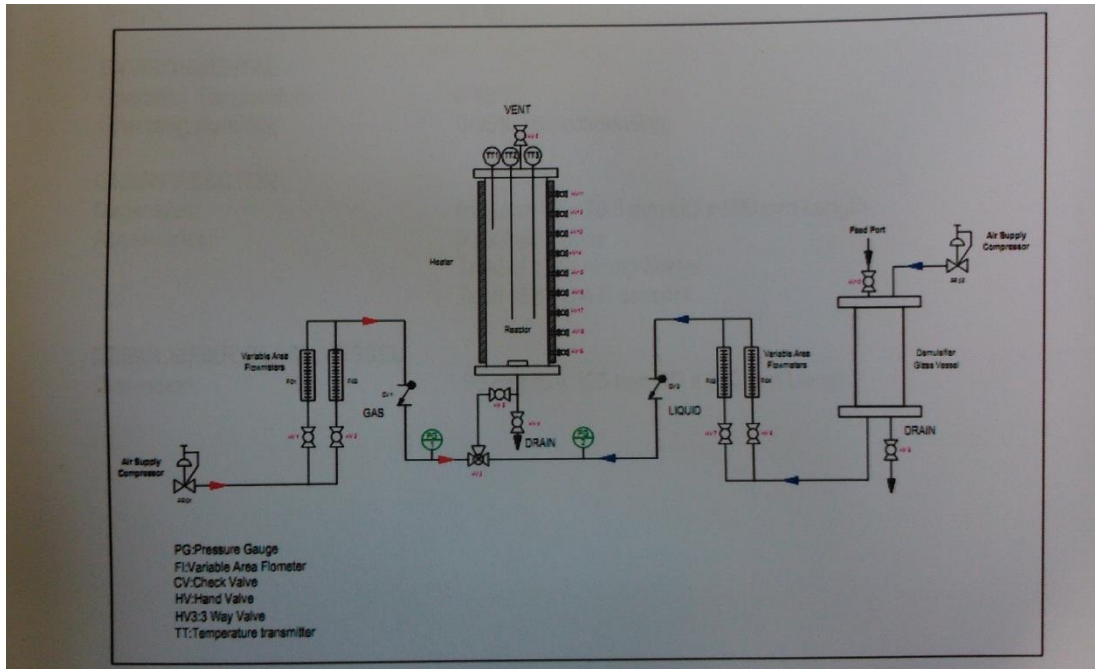
Figure 5: SOLTEQ Gas Bubble Emulsion Unit Process Schematic Diagram

Different orifice could be utilized i.e. Ø1mm, Ø 3mm and Ø6mm and the aeration could be achieved at various rates of 50cc/min up to 200 cc/min.

Upon demulsification, bottle tests will be performed immediately to quantify the separation process. Observation will be conducted at time intervals of 5 min, 15 min, 30 min, 1 hour, 2 hour, 4 hour and daily until a week in accordance to ASTM standard D1401 – 09: Standard Test Method for water separability of petroleum oils and synthetic fluids.

3.2.5 Bubble Size Measurements

The experiment to determine the bubble size is carried out in order to calculate the hydrodynamic forces delivered by the bubbles to the liquid. However, the opaque nature of the MIRI crude emulsion prevent the observation of the bubble as it is too cloudy. Thus, it is replaced by a cooking oil with have the same average viscosity of the MIRI crude and the brown rag layer. The cooking oil is chosen as a substitute as it gives clear vision to the rising bubbles.

The image and video is captured by using the high definition Nikon Digital SLR camera. The observation is taken by using the three different orifice size; 1mm, 3mm and 6mm respectively. The image taken is scale to 2:1 before taking the measurement of the bubble size. In addition, the distance between the bubbles is also measured in order to calculate the hydrodynamic force. While the time between bubbles can be obtained from the video recorded using the camera.
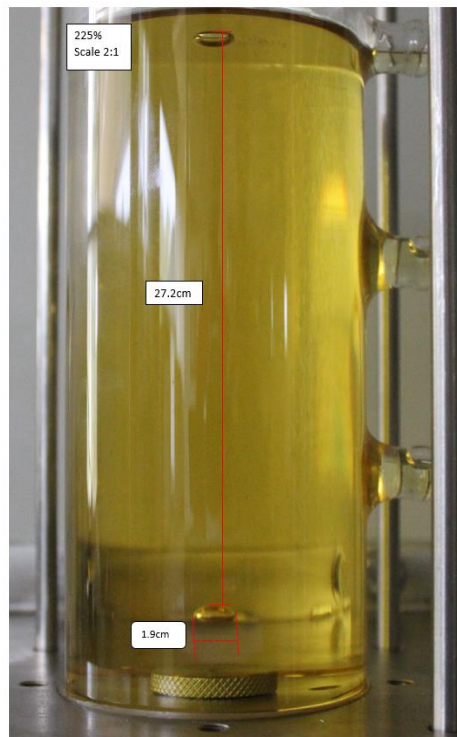
Figure 6: Bubble measurement using 1mm orifice

CHAPTER 4

RESULTS AND DISCUSSION

4.1 Demulsification results

Demulsification processes under 12 different experimental conditions is carried out and three layers were observed during the bottle test. The fraction evolution of volume (%) of each layer was observed and recorded in Table 2. The explanations of the role and effect of each experimental conditions were analysed and discussed in the next section.

4.2 Emulsion, Oil and Water Layer Separation (%) using Ø1mm, Ø3mm and Ø6mm

Based on the Figure 7-9, the role of different aeration rate is observed based on the percentage of emulsion produced with respect to time at 50cc/min, 100cc/min, 150cc/min and 200cc/min respectively. The trend clearly showed that the lower aeration rate would give the highest separation rate which can be observed from the percentage of the lowest emulsion layer at the 30th minute of observation time approximately 25% using 1mm to only 39% (in average) using 3mm and 43% using 6mm. It contradicts the theory that aeration would speed up the separation process by improving the flocculation rate between the droplets. The reason of this would be explained by the role of the hydrodynamic energy given by the bubble size. At lower aeration rate, the lower bubble size would give higher hydrodynamic force that help the flocculation process as mention by (Woodrow et. al., 2006).

The overall trend of the graph provides the relationship between the emulsion layer volume percentage and the bubble size. The graph using 1mm orifice give a steep decreasing curve of the emulsion layer from the highest 93% to 25% at 30th minute and manage to separate the emulsion layer at 68% difference. Meanwhile, the graph using 3mm and 6mm orifice gives out a linear and a combination of steep and linear shape respectively. At 30th minute, both of the graph indicate 55% and 57% emulsion layer differences, respectively. The highest emulsion separation percentage is the lowest orifice diameter. It is believed that the reason of this was due to the role of the bubble size. At lower bubble size, the presence of hydrodynamic forces promote the flocculation rate between the crude droplets. This was supported by the result using 1mm orifice where the percentage of emulsion layer is the smallest at low aeration rate.

(a)

(b)

24

Emulsion Layer (%) vs Periodic Bottle Test using Ø6mm orifice
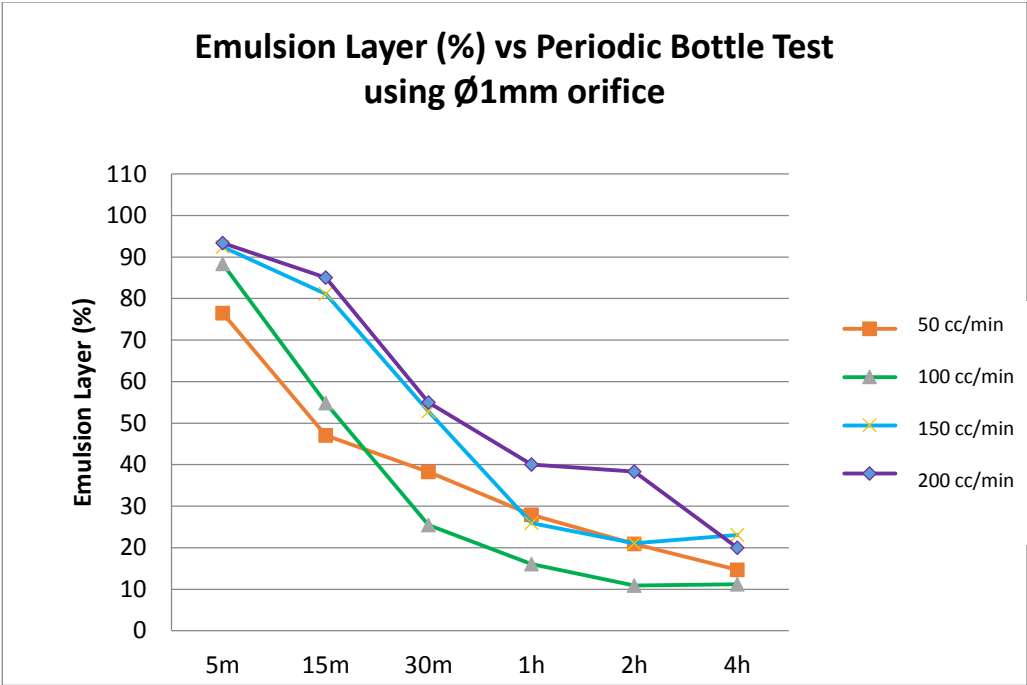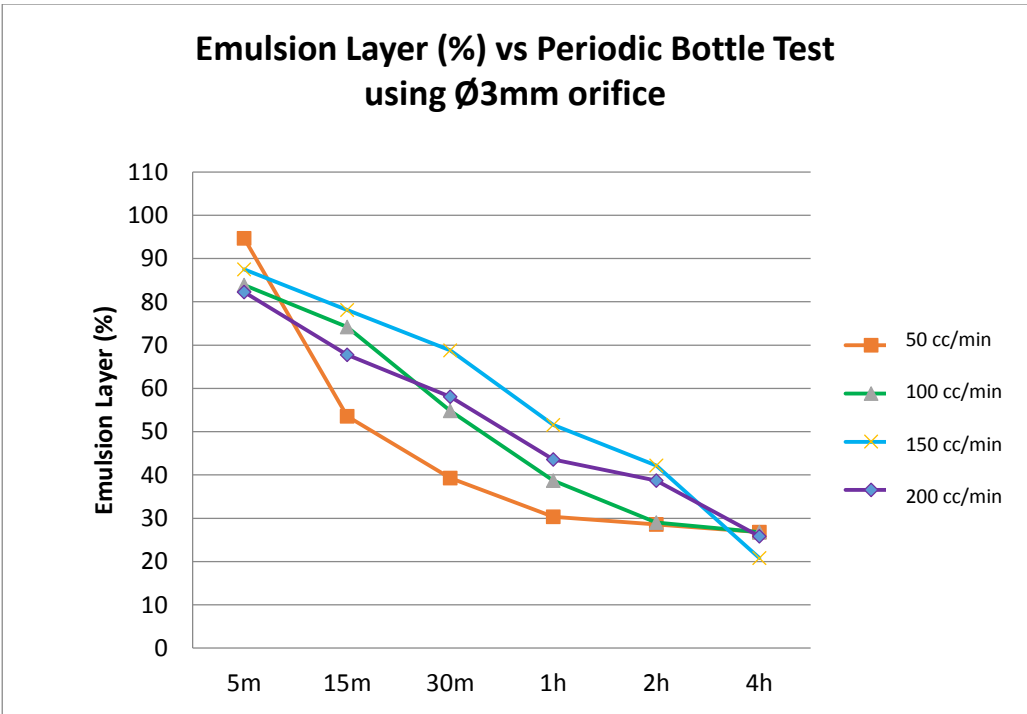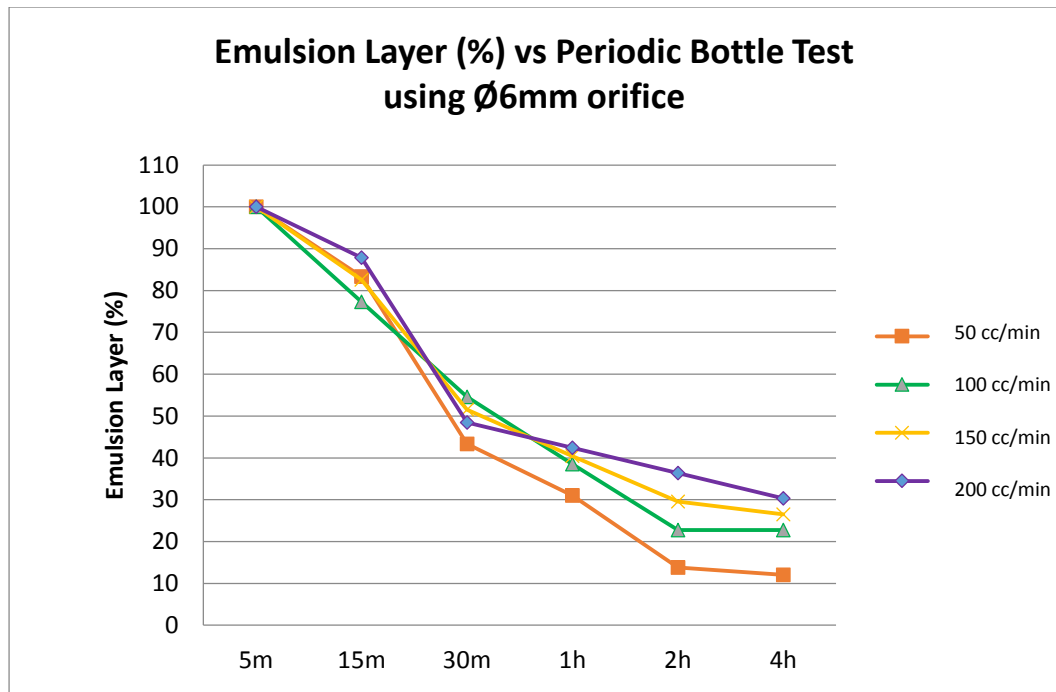
(c)

Figure 7: Emulsion Layer (%) Separated at respective aeration rate using,

a) 1mm orifice, b) 3mm orifice, and c) 6mm orifice

In order to analyse the role of the aeration rate and the bubble size, percentage of volume of oil and water layer separated during the bottle test under different aeration rate and orifice diameter can be observed in the Figure 7-9 at a controlled temperature 60°C. The higher aeration rate would slow down the separation process which can be observed from the percentage volume of oil and water separated at the 30th minute observation time with approximately 56% using 6mm to 50% using 3mm and only 54% using 1mm. The aeration rate of 50 cc/min give the highest amount of oil separated for all three orifice sizes. Moreover, for the water layer percentage volume graph, about 12% to 30% water layer is separated using 3mm and 1mm respectively. Only 13% water layer is separated using 3mm. It is also observed that the highest water separated at 30th minute for all three orifice were achieved at 100cc/min. Similar results and trend is observed for the emulsion layer separation graph. Accordingly, the low aeration rate of 100cc/min contradict the theory that higher aeration rate would increase the separation rate. It was believed that the reason for this is the same where the separation rate were mainly induce by the hydrodynamic force provided by the bubbles (Woodrow et. al., 2006). Hence, the hydrodynamic forces imposed by the bubble size can alter the separation performance of the W/O emulsion.

(a)

(b)

27
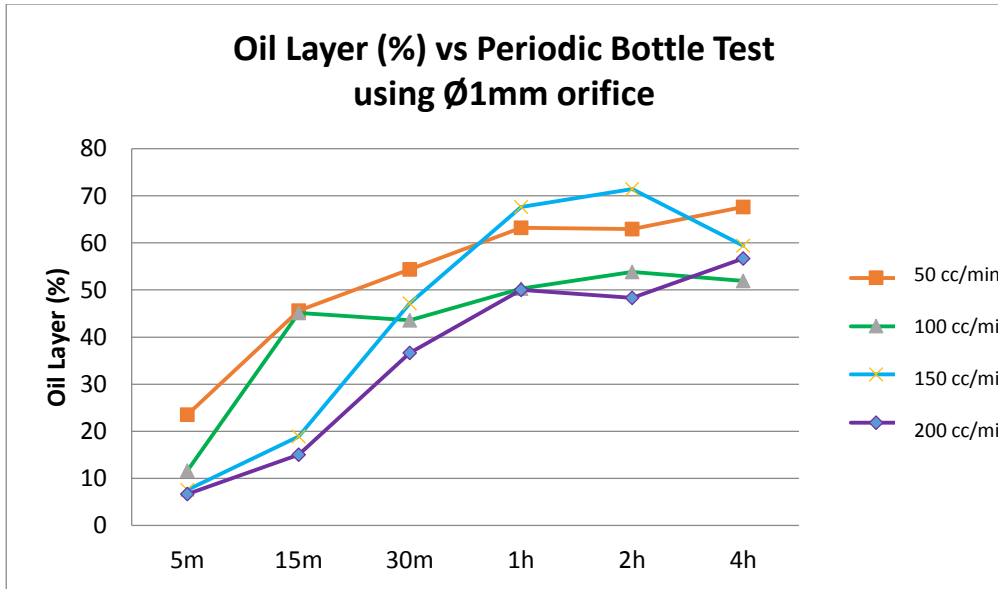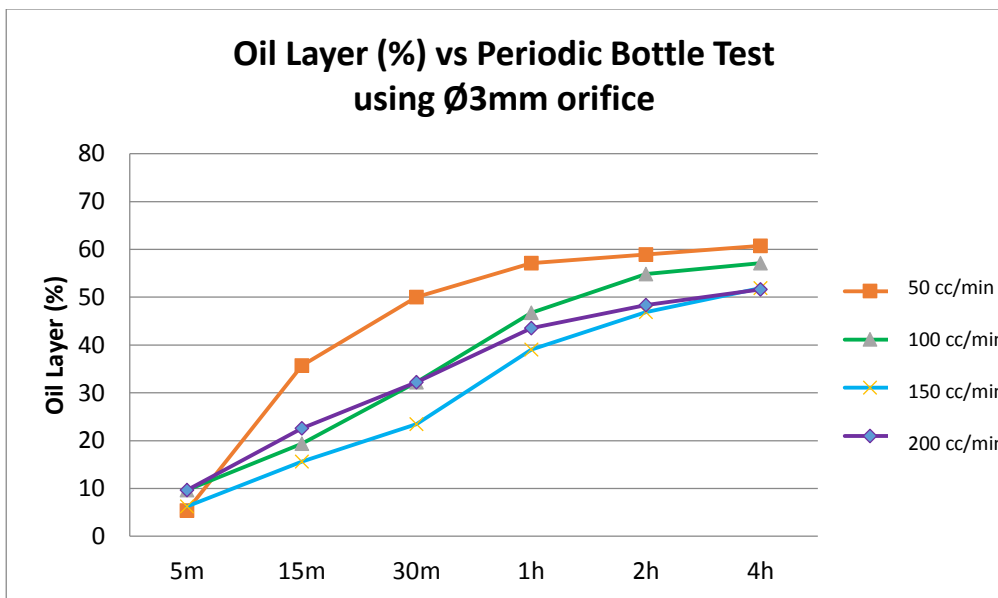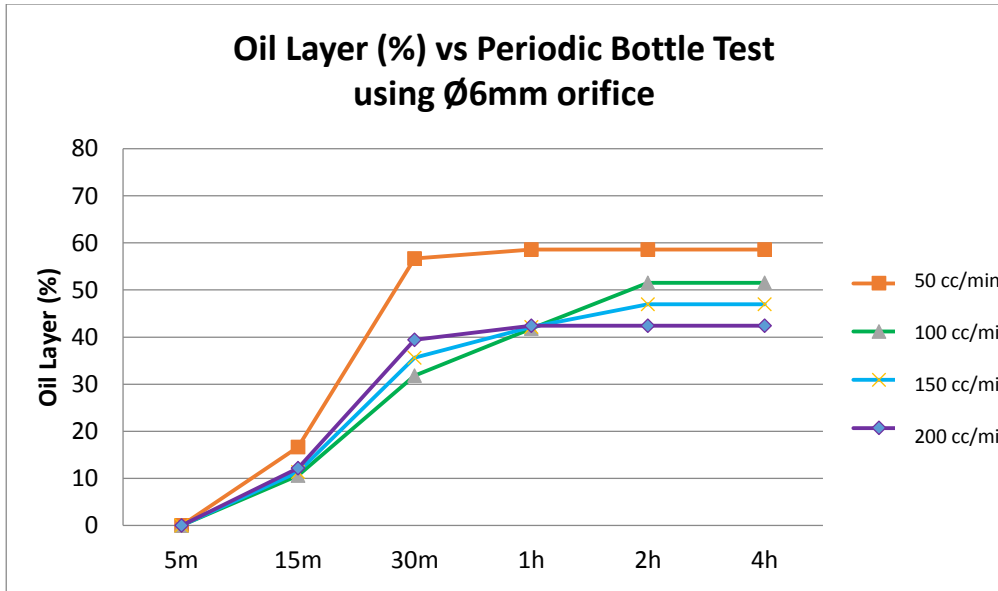
(c)

Figure 8: Oil Layer (%) Separated at respective aeration rate using,
1mm orifice, b) 3mm orifice, and c) 6mm orifice

(a)

(b)
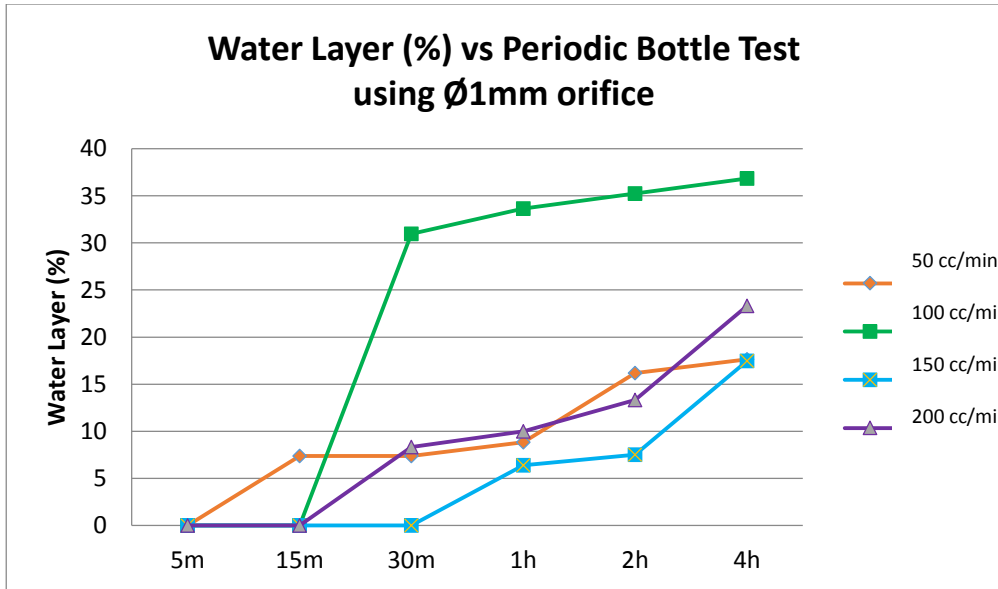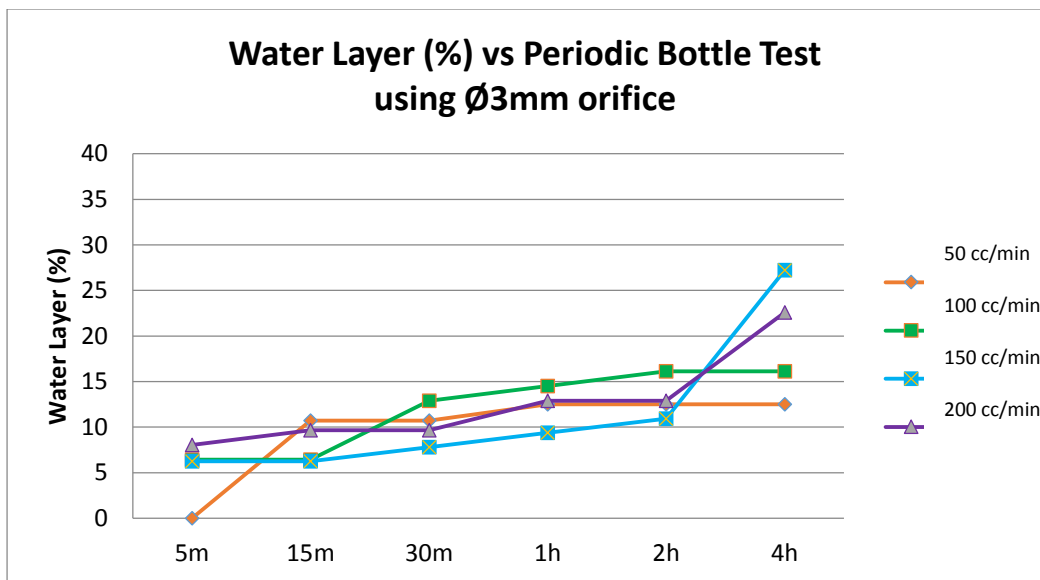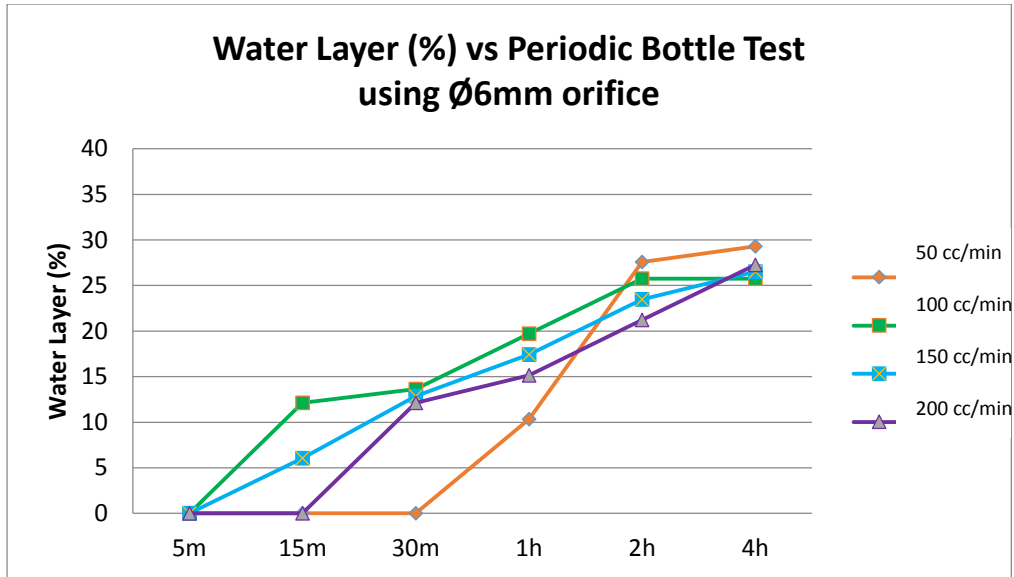
Figure 9: Water Layer Separation (%) at respective aeration rate using,

a) 1mm orifice, b) 3mm orifice, and c) 6mm orifice

Table 2: Observation Data of Percentage Volume of Each Layer during Bottle Test

Run No.	Orifice Diameter (mm)	Aeration (cc/min)	BOTTLE TEST - OBSERVATION TIME																
			5min.			15min.			30min.			1h			2h			4h		
			Oil	Emulsion	Water	Oil	Emulsion	Water	Oil	Emulsion	Water	Oil	Emulsion	Water	Oil	Emulsion	Water	Oil	Emulsion	Water
1	1	50	23.53	76.47	0.00	45.59	47.06	7.35	54.41	38.24	7.35	63.24	27.94	8.82	62.94	20.88	16.18	67.65	14.71	17.65
2		100	11.61	88.39	0.00	45.16	54.84	0.00	43.55	25.48	30.97	50.32	16.03	33.65	53.85	10.90	35.26	51.92	11.22	36.86
3		150	7.55	92.45	0.00	18.87	81.13	0.00	47.17	52.83	0.00	67.67	25.94	6.39	71.43	21.05	7.52	59.44	23.08	17.48
4		200	6.67	93.33	0.00	15.00	85.00	0.00	36.67	55.00	8.33	50.00	40.00	10.00	48.33	38.33	13.33	56.67	20.00	23.33
5	3	50	5.36	94.64	0.00	35.71	53.57	10.71	50.00	39.29	10.71	57.14	30.36	12.50	58.93	28.57	12.50	60.71	26.79	12.50
6		100	9.68	83.87	6.45	19.35	74.19	6.45	32.26	54.84	12.90	46.77	38.71	14.52	54.84	29.03	16.13	57.10	26.77	16.13
7		150	6.25	87.50	6.25	15.63	78.13	6.25	23.44	68.75	7.81	39.06	51.56	9.38	46.88	42.19	10.94	51.92	20.83	27.24
8		200	9.68	82.26	8.06	22.58	67.74	9.68	32.26	58.06	9.68	43.55	43.55	12.90	48.39	38.71	12.90	51.61	25.81	22.58
9	6	50	0.00	100.00	0.00	16.67	83.33	0.00	56.67	43.33	0.00	58.62	31.03	10.34	58.62	13.79	27.59	58.62	12.07	29.31
10		100	0.00	100.00	0.00	10.61	77.27	12.12	31.82	54.55	13.64	41.82	38.48	19.70	51.52	22.73	25.76	51.52	22.73	25.76
11		150	0.00	100.00	0.00	11.36	82.58	6.06	35.61	51.52	12.88	42.12	40.45	17.42	46.97	29.55	23.48	46.97	26.52	26.52
12		200	0.00	100.00	0.00	12.12	87.88	0.00	39.39	48.48	12.12	42.42	42.42	15.15	42.42	36.36	21.21	42.42	30.30	27.27

4.3 Effect of Aeration rate and Bubble Size on Hydrodynamic Forces

It is observed that all of the bubble have the same ellipsoidal-like shape and rising in a straight path. As discussed by Wu and Gharib (2002), the smaller diameter capillary tube will give the ellipsoid shape instead of spherical shape. As for the velocity, the experiment also agreed with the results given by Wu and Gharib (2002). Smaller capillary tube has bubble curvature at detachment point as shown in Figure 8. Higher velocity is produced by the propulsion when the bubble detached. The bubble average travelling velocity are 0.136 m/s, 0.1233 m/s and 0.2094 m/s (large bubble) for 1mm, 3mm and 6mm orifice respectively. The 6mm orifice also produces small bubbles travelling at 0.133 m/s.

Increasing aeration rate is insignificant to the demulsification performance and has tendency to hinder oil-water separation process as presented in Figure 4-6. It means that the optimum aeration rate is 50cc/min and 100 cc/min and it is adequate to give maximum performance in separation process by enhancing the role of flocculation and coalescence of the droplets. Under high aeration rate, the performance of separation is reduced for all the fraction volume layer. Furthermore, the smaller orifice diameter of 1mm give higher separation performance as compared to the higher orifice diameter (3mm and 6mm). The main reason for this was expected to be due to the effect of the hydrodynamic forces given by the bubble size. The increasing flocculation rate of droplets given by applying additional source (the bubble) driving the flocculation and also coalescence (Schramm, 2005). Based on these argument, the aeration rate required would be lower due to the hydrodynamic force exert by the different bubble size. Moreover, it can be observed that the higher bubble size with higher aeration rate would slower the emulsion separation rate. As the aeration rate increases, the hydrodynamic forces imposed by the bubble size would prevent flocculation and coalescence between droplets.

The kinetic energy of 1mm diameter bubble can be obtained by the following calculations and the summary is given in Table 3,

1) The equivalent diameter is calculated for the oblate ellipse

Area:

A = π a b / 4

   = π (0.01) (0.00475) / 4

   = 3.73 x 10⁻⁵ m²

Perimeter:

$$P = 2\pi \left(\frac{\left(\frac{a}{2}\right)^2 + \left(\frac{b}{2}\right)^2}{2} \right)^{\frac{1}{2}}$$

$$P = 2\pi \left(\frac{\left(\frac{0.01}{2}\right)^2 + \left(\frac{0.00475}{2}\right)^2}{2} \right)^{\frac{1}{2}}$$

$P = 1.739 \times 10^{-2} \, m$

Equivalent Diameter (De):

De = 1.55 A⁰·⁶²⁵ / P⁰·²⁵

   = 1.55 (3.73 x 10⁻⁵)⁰·⁶²⁵ / (1.739× 10⁻²)⁰·²⁵

   = **0.0073 m**

2) Aspect ratio, X;

$$X_{(R)} = 2.18R - 0.1$$

$$X_{(R)} = 2.18(0.0073) - 0.1$$

$$\boldsymbol{X_{(R)} = -0.084}$$

3) G(X)

$$G(X) = \frac{\frac{1}{3}X^{\frac{4}{3}}(X^2-1)^{\frac{3}{2}}\left[(X^2-1)^{\frac{1}{2}}-(2-X^2)sec^{-1}X\right]}{\left[X^2sec^{-1}X-(X^2-1)^{\frac{1}{2}}\right]^2}$$

$$= \frac{\frac{1}{3}(-0.084)^{\frac{4}{3}}((-0.084)^2-1)^{\frac{3}{2}}\left[((-0.084)^2-1)^{\frac{1}{2}}-(2-(-0.084)^2)sec^{-1}(-0.084)\right]}{\left[(-0.084)sec^{-1}(-0.084)-((-0.084)^2-1)^{\frac{1}{2}}\right]^2}$$

$$G(X) = 3.685$$

4) From the table by Moore (1965), the value of H(X) of $X_{(R)} = 2.11$ is

-0.138

Table 3: H(X) value (Moore, 1965)

χ	$H(\chi)$	χ	$H(\chi)$
1·0	− 2·211	2·6	+ 1·499
1·1	− 2·129	2·7	+ 1·884
1·2	− 2·025	2·8	+ 2·286
1·3	− 1·899	2·9	+ 2·684
1·4	− 1·751	3·0	+ 3·112
1·5	− 1·583	3·1	+ 3·555
1·6	− 1·394	3·2	+ 4·013
1·7	− 1·186	3·3	+ 4·484
1·8	− 0·959	3·4	+ 4·971
1·9	− 0·714	3·5	+ 5·472
2·0	− 0·450	3·6	+ 5·987
2·1	− 0·168	3·7	+ 6·517
2·2	+ 0·131	3·8	+ 7·061
2·3	+ 0·448	3·9	+ 7·618
2·4	+ 0·781	4·0	+ 8·189
2·5	+ 1·131		

Reynold's number

$$Re = \frac{2RU}{v}$$

$$Re = \frac{2(0.0095)(0.1432)}{0.073}$$

$$Re = 73.902$$

34

5) The drag coefficient can be found by,

$$C_D = \frac{48}{Re}G(X) + \frac{48}{Re^{\frac{3}{2}}}G(X)H(X)$$

$$C_D = \frac{48}{34.290}(3.685) + \frac{48}{34.290^{\frac{3}{2}}}(3.685)(2.684)$$

$$\boldsymbol{C_D = 2.355}$$

6) Thus, the buoyant force and drag force are

$$F_B = (\rho_l - \rho_g)Vg$$

$$F_B = (920 - 1.225)(0.1654\mu)(9.81)$$

$$\boldsymbol{F_B = 0.00224\mu N}$$

$$F_D = 0.5C_D\pi R^2(\rho_l - \rho_g)U^2$$

$$F_D = 0.5(7.523)\pi(0.0073)^2(918.775)(0.1432)^2$$

$$\boldsymbol{F_D = -0.0028\ \mu N}$$

$$\boldsymbol{\therefore F_B \approx -F_D}$$

7) Lastly, the kinetic energy delivered to the fluid as the bubble rises,

$$E_k = F_B \cdot U$$

$$E_k = 0.00224\mu N \cdot 0.1236$$

$$\boldsymbol{E_k = 277.2\mu W}$$

Table 4: Kinetic Energy for each of the bubble size

Orifice	Major Axis Diameter (m)	Minor Axis Diameter (m)	Velocity (m/s)	Kinetic Energy, E_k
1mm	0.01	0.00475	0.1236	277.2 µW
3mm	0.0075	0.00365	0.1233	119.5 µW
6mm	0.01125	0.00475	0.2094	333 µW
	0.00575	0.00345	0.1333	
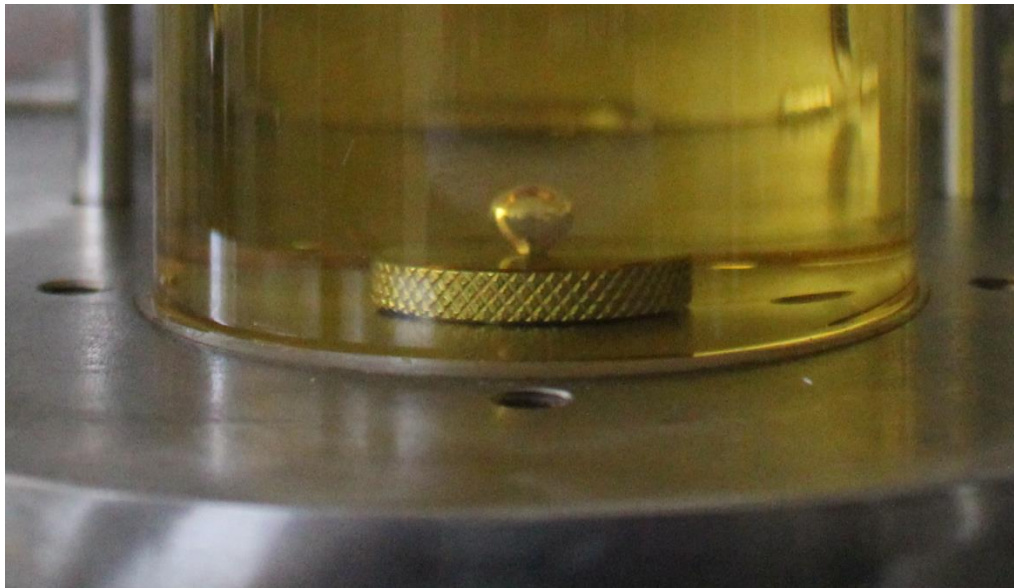
Figure 10: Bubble curvature detachment point from 1mm orifice

Table 5: Summary of the Kinetic Energy Calculation

Orifice	Major diameter (m)	Minor diameter (m)	distance between bubble (m)	Time between bubbles (s)	velocity (m/s)	Area (m^2)	Perimeter (m)	Equivalent Diameter, De (m)
1mm	0.01	0.00475	0.1360	1.10	0.1236	3.731E-05	1.739E-02	0.0073
3mm	0.0075	0.00365	0.0555	0.45	0.1233	2.150E-05	1.310E-02	0.0055
6mm	0.01125	0.00475	0.0890	0.43	0.2094	4.197E-05	1.918E-02	0.0077
	0.00575	0.00345	0.0550	0.41	0.1333	1.558E-05	1.053E-02	0.0048

Ratio, (major: minor)	χ (From Table)	Vol of bubble (oblate ellipsoid), m3	Viscosity (Pa.s)	density oil, ρL (kg/m3)	density air, ρg (kg/m3)	ρL-ρg (kg/m^3)
2.11	-0.138	2.48709E-07	0.03	896.6	1.225	918.775
2.05	-0.309	1.07501E-07	0.03	896.6	1.225	918.775
2.37	0.681	3.14773E-07	0.03	896.6	1.225	918.775
1.67	-1.248	5.97246E-08	0.03	896.6	1.225	918.775

Aspect Ratio, Xr	G(X)	Re	Cd	Drag Force, Fd (µN)	Buoyant Force, Fb (µN)	Kinetic Energy, Ek (W)	
-0.084	3.685	73.902	2.355	-0.0028	0.00224	2.772E-04	
-0.088	2.459	55.290	2.046	-0.0014	0.00097	1.195E-04	
-0.083	2.719	140.819	0.980	-0.0036	0.00284	5.941E-04	3.33E-04
-0.090	2.719	45.826	2.323	-0.0014	0.00054	7.177E-05	
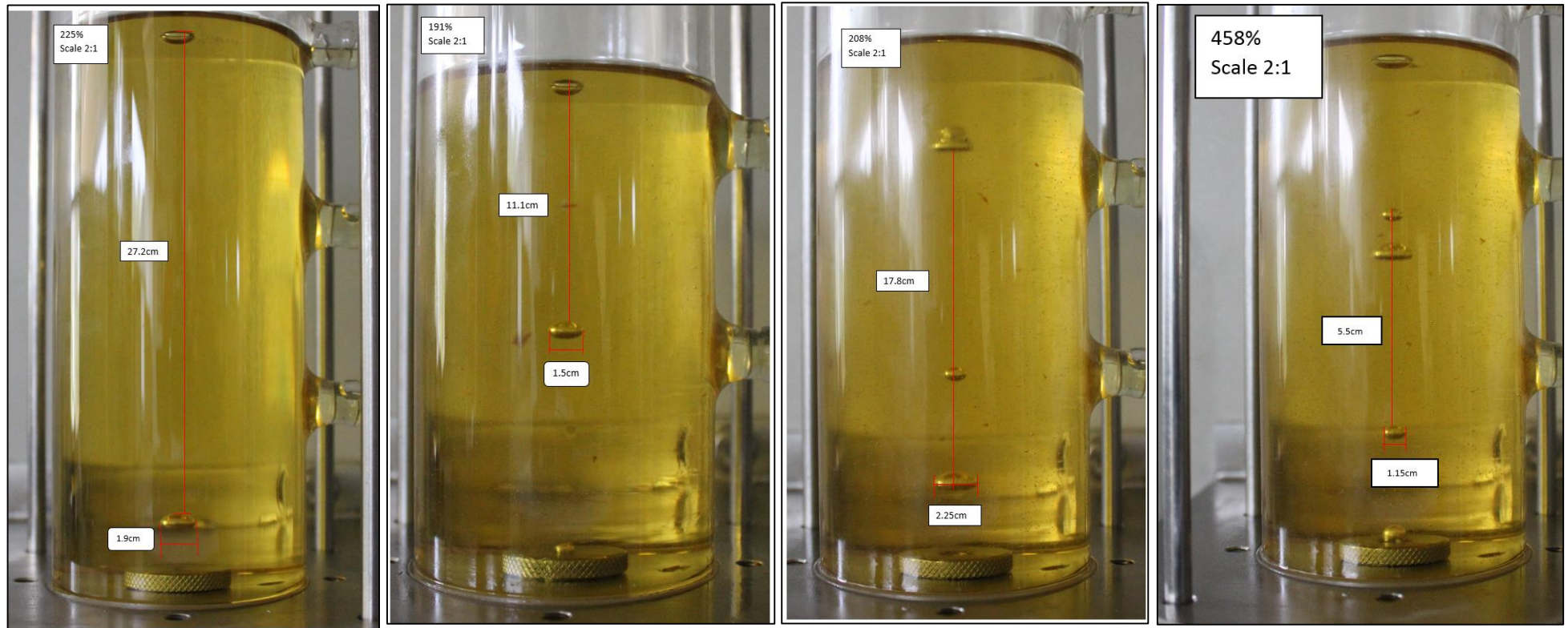
Figure 11: Bubble Measurement for each of orifice;

(a)1mm, (b)3mm, (c)6mm – big bubble and (d) 6mm – small bubble

CHAPTER 5:

CONCLUSION AND RECOMMENDATION

4.1 Conclusion

The findings of the experiments have successfully explore and investigate the performance of aeration rate and the effect of the bubble size to the emulsion. The aeration would help the emulsion breaking by promoting an increase in flocculation rate between the droplets which lead to coalescence. However, it can be concluded that intense rate of aeration could give opposite effect by decreasing the rate of the separation for the three layers; oil, water and emulsion.

Moreover, the various sizes of bubble diameter will have a different hydrodynamic effect to the liquid. As the bubbles rises, it exhibit hydrodynamic force to the liquid which further affect the demulsification rate. Thus, the hydrodynamic force and the aeration affects separation rate of the three layers. Hydrodynamic force of bubble would reduce the need of aeration since it enhances the flocculation rate by giving kinetic energy to the droplets as it rises. It is supported by the experiment result of 1mm diameter bubble that has highest kinetic energy of 2.77W which also gives highest separation rate for oil, water and emulsion layer.

The experiment gives an insight on the best aeration rate to demulsify the emulsion. The best aeration rate is 100cc/min using 1mm diameter observed at the critical 30th minutes. The optimum solution would give approximately 47% oil fraction 30% water fraction and only 25% emulsion layer. As the objective of the project is to study the separation behavior of MIRI crude emulsion under different aeration variables and to assess the bubble size effect to resolve the emulsion, thus the objectives are achieved.

4.2 Recommendation

The emulsion is common in the production of the crude. The experiment can be further expanded by using other crude emulsions as different crude consists of different properties. The comparison and the similarities of the results can give the separation rate of different crude to be explored. Furthermore, besides the demulsification test rig unit, the experiment can further analyzed by using the gas flotation unit which include the bubble size analyzer. It is also recommended to use a high precision camera to capture the quality image and the trajectory of the rising bubbles as well as to see in a different angle.

Furthermore, it is recommended to expand the tests by using different orifice diameter to validate the data gathering. These test will verify the demulsification quality of the crude which is more detailed and accurate. Improvement of the demulsification test rig device. The demulsification test rig device can also be improved to increase its parameter control and user friendly. Thus, further evaluation on the equipment can be conducted with series of pilot test experiments. Further study on the bubble size can be carried out by using different viscosity of oil to investigate the behavior and hydrodynamic forces toward aeration treatment.

REFERENCES

[1] D. Nikolov, M. Randie, C. S. Shetty, D. T. Wasan (1996), *Chemical Demulsification of Oil-In-Water Emulsion Using Air-Flotation: The Importance of Film Thickness Stability*, Chemical Engineering Communications

[2] Balasubramanian Ramakrishnan, Mallavarapu Megharaj, Kadiyala Venkateswarlu, Ravi Naidu, Nambrattil Sethunathan (2010), *The Impacts of Environmental Pollutants on Microalgae and Cyanobacteria*, Critical Reviews in Environmental Science and Technology

[3] Becher, P. (2001). *Emulsions, Theory and Practice*, 3rd ed.; Oxford University Press: New York; 2001.

[4] Fingas M. (2005), *Stability and Resurfacing of Dispersed Oil, Environmental Technology* Center, Environment Canada.

[5] H.B. Bradley ed. 1987. *Petroleum Engineering Handbook*, 19-26. Richardson, Texas: SPE.

[6] Helko Borsdorf, Thomas Mayer, Mashaalah Zarejousheghani, Gary A. Eiceman (2011), *Recent Developments in Ion Mobility Spectrometry*, Applied Spectroscopy Reviews

[7] C. Sharma, I. Haque, S. N. Srivastava (1982), *Chemical demulsification of natural petroleum emulsions of Assam (India)*, Colloid and Polymer Science

[8] Ivanov B, (1999), *Flocculation and coalescence of micron-size emulsion droplets*, New Jersey, Elsevier

[9] Mingming Wu and Gharib M. (2002). Experimental Studies on the Shape and Path of Small Air Bubbles Rising in Clean Water. Physics of Fluids, Volume 14:7.

[10] Moore D.W. (1965). *The velocity of rise of distorted gas bubbles in a liquid of small viscosity*. J. Fluid Mechanics, Volume 23:4, pp 749-766.

[11] Schramm Laurier L. (2005), *Emulsions, Foams and Suspensions: Fundamentals and Applications,* Wiley-VCH

[12] Woodrow L. et al. (2006) *Force Measurement on Rising Bubbles*. Laboratoire de Physique

APPENDIX

Appendix A: Gantt Chart (FYP I)

NO	SUBJECT	TIME	SEMESTER 1 (FYP I)													
			1	2	3	4	5	6	7	8	9	10	11	12	13	14
1	Selection of FYP Topic	1st Briefing	█													
2	Project Introduction	23/9/2014		█												
3	Extended Proposal Preparation	29/9/2014														
	• Literature Reviews	3 Weeks			█	█	█									
	• Project Methodology Planning	3 Weeks			█	█	█									
	• Project Gantt Chart & Milestones Scheduling	1 Weeks					█									
	• Industry Case Study	3 Weeks				█	█	█								
4	Lab Apparatus Familiarization	1 Weeks						█								
5	Submission of Extended Proposal	5/11/2014-7/11/2014						▓								
6	Proposal Defense Preparation	1 Weeks							█							
7	Proposal Defense	17/11/2014 - 21/11/2014								▓	▓					
8	Preparation of Experiments	3 Weeks														
	• Formation of Synthetic Water Preparation	1 Week									█					
9	MIRI Crude Emulsion Demulsification Evaluation & Experiments	4 Weeks														
	• Demulsification MIRI Crude Familiarization	1 Week										█				
	• Demulsification Test – Aeration (Ø 1mm & Ø 3mm) - 50cc/min, 100cc/min , 150cc/min, 200cc/min	4 Weeks										█	█	█	█	
	• Demulsification Test - Bottle Test Monitoring	4 Weeks										█	█	█	█	
10	Submission of Interim Draft Report	19/12/2014													▓	
11	Submission of Interim Report	26/12/2014														▓

Appendix B: Gantt Chart (FYP II)

NO	SUBJECT	TIME	SEMESTER 2 (FYP II)													
			1	2	3	4	5	6	7	8	9	10	11	12	13	14
1	**Preliminary Data Analysis for Phase I Experiments**	**1 Weeks**	G													
2	**MIRI Crude Demulsification Evaluation & Experiment**	**5 Weeks**														
	• Demulsification Test – Aeration (Ø 3mm & Ø 5mm) - 50cc/min, 100cc/min , 150cc/min, 200cc/min	5 Weeks		G	G	G	G	G								
	• Demulsification Test - Bottle Test Monitoring	5 Weeks		G	G	G	G	G								
	• Time Separation Comparison	2 Weeks					G	G								
3	**Preliminary Data Analysis for Phase II Experiments**	**2 Weeks**						G	G							
4	**Preparation of Progress Report**	**2 Weeks**						G	G							
5	**Submission of Progress Report**	**1 Week**							Y							
6	**Project Analyses & Discussion**	**6 Weeks**														
	• Comparative Analyses on the Settling Period for Complete Emulsion Separations	1 Week								G	G	G	G	G	G	
	• Comparative Analyses on the Separated Water/Oil Volume	1 Week								G	G	G	G	G	G	
	• Setting up of Recommended Operating Conditions for Effective Stable Emulsion preparation	1 Week								G	G	G	G	G	G	
	• Cost Engineering Analyses	1 Week								G	G	G	G	G	G	
	• Compilation of Project Analyses and Discussion	1 Week													G	
7	**PRE-SEDEX**	**1 Week**									Y					
8	**Preparation of Draft Report & Technical Paper**	**4 Weeks**									G	G	G			
9	**Submission of Draft Report**	**1 Week**											Y			
10	**Submission of Technical Paper**	**1 Week**												Y		

11	**Submission of Dissertation (Soft Bound)**	1 Week														🟨		
12	**Oral Presentation / Viva**	1 Week															🟨	
13	**Submission of Project Dissertation (Hard Bound)**	1 Week																🟨

Appendix C: Experiment Run Table

Orifice Diameter	1mm				3mm				6mm			
Aeration (cc/min)	50	100	150	200	50	100	150	200	50	100	150	200
Experiment Day												
W10 Friday (28/11/2014)	Run1											
W11 Monday(01/12/2014)		Run2	Run3	Run4								
W12 Friday (12/12/2014)					Run5	Run6	Run7	Run8				
W14 Friday (26/12/2014)									Run9	Run10	Run11	Run12

Legend:

🟩 Completed

🟧 Ongoing

🟨 Pending

Appendix D: MIRI Crude Demulsification Results

Using 1mm Orifice Diameter

Run 1: Rate of Aeration – 50cc/min

Time	Oil	Emulsion	Water
5m	23.52941	76.47059	0
15m	45.58824	47.05882	7.352941
30m	54.41176	38.23529	7.352941
1h	63.23529	27.94118	8.823529
2h	62.94118	20.88235	16.17647
4h	67.64706	14.70588	17.64706
1d	70.05988	10.47904	19.46108
2d	70.90909	7.878788	21.21212
3d	71.875	7.8125	20.3125
4d	71.875	7.8125	20.3125
5d	69.84127	6.349206	23.80952
6d	69.84127	6.349206	23.80952
7d	69.35484	6.451613	24.19355

Run 2: Rate of Aeration – 100cc/min

Time	Oil	Emulsion	Water
5m	11.6129	88.3871	0
15m	45.16129	54.83871	0
30m	43.54839	25.48387	30.96774
1h	50.32051	16.02564	33.65385
2h	53.84615	10.89744	35.25641
4h	51.92308	11.21795	36.85897
1d	54.69799	6.711409	38.5906
2d	55.9322	5.084746	38.98305
3d	55.17241	5.172414	39.65517
4d	55.17241	5.172414	39.65517
5d	55.17241	5.172414	39.65517
6d	54.42177	5.102041	40.47619
7d	54.42177	5.102041	40.47619

Run 3: Rate of Aeration – 150cc/min

Time	Oil	Emulsion	Water
5m	7.54717	92.45283	0
15m	18.86792	81.13208	0
30m	47.16981	52.83019	0
1h	67.66917	25.93985	6.390977
2h	71.42857	21.05263	7.518797
4h	59.44056	23.07692	17.48252
1d	72.30769	14.23077	13.46154
2d	71.76471	14.5098	13.72549
3d	73.72549	5.882353	20.39216
4d	72.94118	5.882353	21.17647
5d	70.4	8	21.6
6d	72.4	6	21.6
7d	72.4	6	21.6

Run 4: Rate of Aeration – 200cc/min

Time	Oil	Emulsion	Water
5m	6.666667	93.33333	0
15m	15	85	0
30m	36.66667	55	8.333333
1h	50	40	10
2h	48.33333	38.33333	13.33333
4h	56.66667	20	23.33333
1d	58.62069	13.7931	27.58621
2d	59.64912	10.52632	29.82456
3d	58.92857	10.71429	30.35714
4d	58.92857	10.71429	30.35714
5d	58.92857	10.71429	30.35714
6d	60.71429	8.928571	30.35714
7d	60.71429	8.928571	30.35714

Using 3mm Orifice Diameter

Run 1: Rate of Aeration – 50cc/min

Time	Oil	Emulsion	Water
5m	5.357143	94.64286	0
15m	35.71429	53.57143	10.71429
30m	50	39.28571	10.71429
1h	57.14286	30.35714	12.5
2h	58.92857	28.57143	12.5
4h	60.71429	26.78571	12.5
1d	63.15789	12.2807	24.5614
2d	63.15789	12.2807	24.5614
3d	67.92453	7.54717	24.5283
4d	69.23077	5.769231	25
5d	69.23077	5.769231	25
6d	68.62745	7.843137	23.52941
7d	68.62745	7.843137	23.52941

Run 2: Rate of Aeration – 100cc/min

Time	Oil	Emulsion	Water
5m	9.677419	83.87097	6.451613
15m	19.35484	74.19355	6.451613
30m	32.25806	54.83871	12.90323
1h	46.77419	38.70968	14.51613
2h	54.83871	29.03226	16.12903
4h	57.09677	26.77419	16.12903
1d	61.01695	16.94915	22.0339
2d	67.92453	9.433962	22.64151
3d	62.06897	13.7931	24.13793
4d	61.41975	15.78283	22.79742
5d	62.5	14.28571	23.21429
6d	62.5	12.5	25
7d	64.28571	10.71429	25

Run 3: Rate of Aeration – 150cc/min

Time	Oil	Emulsion	Water
5m	6.25	87.5	6.25
15m	15.625	78.125	6.25
30m	23.4375	68.75	7.8125
1h	39.0625	51.5625	9.375
2h	46.875	42.1875	10.9375
4h	51.92308	20.83333	27.24359
1d	55.12821	14.42308	30.44872
2d	56.45161	14.51613	29.03226
3d	58.06452	11.29032	30.64516
4d	56.66667	11.66667	31.66667
5d	55.17241	12.06897	32.75862
6d	56.89655	10.34483	32.75862
7d	56.89655	10.34483	32.75862

Run 4: Rate of Aeration – 200cc/min

Time	Oil	Emulsion	Water
5m	9.677419	82.25806	8.064516
15m	22.58065	67.74194	9.677419
30m	32.25806	58.06452	9.677419
1h	43.54839	43.54839	12.90323
2h	48.3871	38.70968	12.90323
4h	51.6129	25.80645	22.58065
1d	52.54237	16.94915	30.50847
2d	55.17241	10.34483	34.48276
3d	53.44828	10.34483	36.2069
4d	56.14035	10.52632	33.33333
5d	56.14035	8.77193	35.08772
6d	55.35714	8.928571	35.71429
7d	55.35714	8.928571	35.71429

Using 6mm Orifice Diameter

Run 1: Rate of Aeration – 50cc/min

Time	Oil	Emulsion	Water
5m	0	100	0
15m	16.66667	83.33333	0
30m	56.66667	43.33333	0
1h	58.62069	31.03448	10.34483
2h	58.62069	13.7931	27.58621
4h	58.62069	12.06897	29.31034
1d	58.62069	12.06897	29.31034
2d	58.62069	10.34483	31.03448
3d	59.64912	8.77193	31.57895
4d	58.92857	8.928571	32.14286
5d	58.18182	9.090909	32.72727
6d	60	7.272727	32.72727
7d	58.18182	7.272727	34.54545

Run 2: Rate of Aeration – 100cc/min

Time	Oil	Emulsion	Water
5m	0	100	0
15m	10.60606	77.27273	12.12121
30m	31.81818	54.54545	13.63636
1h	41.81818	38.48485	19.69697
2h	51.51515	22.72727	25.75758
4h	51.51515	22.72727	25.75758
1d	53.84615	15.38462	30.76923
2d	53.84615	9.230769	36.92308
3d	52.38095	9.52381	38.09524
4d	52.38095	9.52381	38.09524
5d	52.38095	9.52381	38.09524
6d	51.6129	9.677419	38.70968
7d	51.6129	9.677419	38.70968

Run 3: Rate of Aeration – 150cc/min

Time	Oil	Emulsion	Water
5m	0	100	0
15m	11.36364	82.57576	6.060606
30m	35.60606	51.51515	12.87879
1h	42.12121	40.45455	17.42424
2h	46.9697	29.54545	23.48485
4h	46.9697	26.51515	26.51515
1d	50.71315	13.47068	35.81616
2d	50.3937	10.23622	39.37008
3d	50.4	9.6	40
4d	50.4	9.6	40
5d	50.4	9.6	40
6d	50	9.677419	40.32258
7d	50.80645	8.870968	40.32258

Run 4: Rate of Aeration – 200cc/min

Time	Oil	Emulsion	Water
5m	0	100	0
15m	12.12121	87.87879	0
30m	39.39394	48.48485	12.12121
1h	42.42424	42.42424	15.15152
2h	42.42424	36.36364	21.21212
4h	42.42424	30.30303	27.27273
1d	47.38562	11.43791	41.17647
2d	46.77419	11.29032	41.93548
3d	48.3871	9.677419	41.93548
4d	48.3871	9.677419	41.93548
5d	48.3871	9.677419	41.93548
6d	48.3871	9.677419	41.93548
7d	50	8.064516	41.93548